Linear and Nonlinear Viscoelasticity of Carbon Black Filled Elastomers: Use of Complementary Rheological Characterizations

C. Barrès, A. Mongruel, M. Cartault, J. L. Leblanc

Laboratoire de Rhéologie et Mise en Œuvre des Polymères, Université Pierre et Marie Curie, 60 Rue Auber, 94408 Vitry sur Seine, France

Received 14 December 2001; accepted 27 March 2002

ABSTRACT: The viscoelastic properties of filled elastomers (uncured styrene–butadiene rubber filled with carbon black) were investigated with two shear rheometers specially designed for the characterization of complex polymer systems. A torsional strain-controlled rheometer [i.e., a rubber process analyzer (RPA)] was used in dynamic and relaxation modes for measuring the storage and loss moduli and the relaxation modulus. A stress-controlled sliding cylinder rheometer (SCR) was operated for the measurement of the creep compliance. Both devices could be operated on a large scale of imposed strains or stresses ranging from the linear viscoelastic regime to the nonlinear viscoelastic regime, and they were complementary in supporting the original viscoelastic behavior of filled elastomers for a wide experimental time range. Moreover, when the measuring ranges of the two apparatus overlapped, a cross-check of the material functions obtained with the RPA or SCR could be successfully carried out. This validation of the data was performed not only in the linear domain of viscoelasticity, with the classical approach of a generalized Maxwell model, but also in the nonlinear domain, with a viscoelastic integral model of type K-BKZ. © 2002 Wiley Periodicals, Inc. J Appl Polym Sci 87: 31–41, 2003

Key words: elastomers; fillers; viscoelastic properties; modeling

INTRODUCTION

Filled elastomers are known to exhibit a complex rheological behavior that reflects interactions between the elastomer and the reinforcing filler, either carbon black or silane-treated silica. This behavior is characterized, in particular, by a high level of nonlinear viscoelasticity. Highly loaded elastomer compounds hardly exhibit a linear domain of viscoelasticity. From an industrial point of view, this has important consequences for the processing flows of such materials. Several theoretical attempts have been made to describe the complicated rheological behavior of filled polymers (see the review in ref. 1), and the modeling of the nonlinear viscoelastic properties of elastomers and their compounds is still a question under study.[2]

Concerning the rheological characterization, conventional parallel-plate or cone-and-plate rheometers are of limited use with elastomers because wall slip may occur, and the loading of the sample into the testing gap is not easy, affecting the repeatability of tests. Other specific features of these materials, such as their high viscosity or their chemical and physical aging, may raise a number of difficulties. For these reasons, it is necessary to develop specific measuring devices and protocols. Such devices are available in our laboratory. One is a strain-controlled shear rheometer [i.e., a rubber process analyzer (RPA)] specifically designed for elastomers and their compounds (RPA 2000, Alpha Technologies).[3] Its design and operating conditions originate from the practice of vulcametry and are, therefore, slightly different from those of conventional rheometers. It can be operated in dynamic or relaxation modes. The second apparatus, used to carry out creep (i.e., stress-controlled) experiments, is a prototype of a sliding cylinder rheometer (SCR), developed in the laboratory[4] and particularly suited for self-supporting materials such as those used in this study. It can also provide viscosity data at very low shear rates. With these two techniques, we are able to characterize the viscoelastic properties of complex materials in shear-stress- or shear-strain-controlled modes, over a wide range of stresses or strains, thereby covering the linear and nonlinear viscoelastic regimes.

The purpose of this article is twofold. First, we show how these two devices are able to characterize the original viscoelastic behavior of uncured carbon black filled elastomers. The results presented in this work are limited to compounds with sufficiently low filler contents so that a domain of linear viscoelasticity can be observed. The transition from the linear viscoelasticity regime to the nonlinear viscoelasticity regime is

Correspondence to: A. Mongruel (mongruel@ccr.jussieu.fr).

Journal of Applied Polymer Science, Vol. 87, 31–41 (2003)

evidenced here not only with respect to the strain (with the RPA) but also with respect to the stress via SCR creep tests, which is less common. Moreover, we show how this behavior is affected by the filler volume fraction. Second, we carry out a cross-check of the data provided by both techniques to evaluate their consistency and validity. This is done with linear and nonlinear viscoelastic models, which are briefly presented. This cross-check is shown to be satisfactory in the time domain in which the experimental time ranges of both techniques overlap. Some limitations appear, however, and are discussed. Beyond the evaluation of the reliability and consistency of our experimental means, this work yields all the viscoelastic functions, in both the linear and nonlinear viscoelasticity domains, required for implementation in numerical codes to simulate the processing flows of typical industrial compounds. However, this last aspect is beyond the scope of this article.

EXPERIMENTAL

Material preparation

All tests were performed with a series of compounds based on an amorphous, emulsion-polymerized styrene–butadiene copolymer (SBR 1500; styrene content = 23.5%, number-average molecular weight = 77,000 g mol^{-1}, weight-average molecular weight = 405,000 g mol^{-1}, unknown branching ratio). Its glass-transition temperature was around −50°C. N330 carbon black (nitrogen adsorption surface area [BET method]: 83 m^2/g) was used as a filler at different concentrations. The carbon black elementary particles had a characteristic dimension of 30 nm. For these compounds, a percolated particle network was evidenced from electrical conductivity measurements for carbon black volume fractions equal or greater than 0.15 (in agreement with earlier works[5]). The percolation threshold, corresponding to the volume fraction at which the particles form a continuous network in the polymer matrix, characterizes the onset of physical gelation. This is associated with significant changes in the rheological properties, particularly with a yield behavior well documented for highly filled elastomers in earlier works (e.g., ref. 6). In this study, we focused on the fluidlike behavior of elastomer compounds, selecting carbon black volume fractions below 0.15 so that no yield behavior would be expected. Three elastomer samples were studied: the pure elastomer and two compounds whose carbon black volume fractions were $\Phi = 0.045$ and $\Phi = 0.123$, respectively. The usual major ingredients of an industrial compound were added, too, but within the limits of simple recipes. Therefore, processing oil, protectors (antiozone and antioxidant), and vulcanization coagents (zinc oxide and stearic acid) were blended with the polymer and carbon black. However, the curing system (sulfur and accelerators) was excluded because we focused on flow properties. The quantities of all components [parts per hundred parts of rubber (phr)] are given in Table I.

TABLE I
Formulation of the SBR/Carbon Black Compounds

Ingredient	phr
SBR 1500	100
N330 carbon black	0, 10, 30 (volume fractions: 0, 0.045, and 0.123)
Zinc oxide	5
Stearic acid	3
Processing oil (aromatic)	5
Antidegradants	3

Mixing was achieved in a Banbury-type internal mixer. To limit the effects of the specific mixing energy (i.e., energy per unit volume of material), which is known to strongly affect rheological properties, we gave all compounds the same specific energy (ca. 1550 MJ/m^3). Immediately after mixing, the batches were cooled and homogenized between the cylinders of an open mill and were sheeted off in the form of approximately 7-mm-thick sheets, from which most samples were directly cut for testing. These sheets were kept in the dark at room temperature for several weeks before sampling to ensure the stabilization of their properties. It must be mentioned that the samples for SCR tests required a second milling, so their thickness came close to 1 mm. To prevent any influence of this remilling, we also kept the SCR samples for several weeks before creep experiments, and the material properties were checked to be identical to those of non-remilled samples before this study.

Shear-strain-controlled rheometry with the RPA

The behavior of linear viscoelastic materials is characterized by functions such as the elastic and loss moduli. These functions are obtained in dynamic testing, from the measurement of the forces and torques developed by the material when subjected to an oscillatory deformation of controlled amplitude and frequency. The RPA 2000 (Alpha Technologies) is a torsional rheometer specially designed to perform such tests on elastomers and their compounds.[3] The testing cavity is closed and operated under pressure (4 MPa) to reduce slip at the wall and to ensure a perfectly controlled loading of the sample. Reproducibility is achieved within ±3%. Another particularity of the RPA is its reciprocal cone geometry (of angle $\alpha = 0.125$ rad and radius $R = 20.6$ mm). The lower cone is moved with a controlled angular rotation θ. The torque transmitted by the deformed sample is measured on the upper cone. The reciprocal cone geome-

try is equivalent to a conventional cone-and-plate geometry as long as the cone angle α is sufficiently small. We have checked that in the RPA this condition is fulfilled, and so the deformation inside the sample can be considered to be viscosimetric with good precision. The standard equations used in cone-and-plate rheometry apply for the shear strain γ, approximately constant throughout the sample and equal to $\gamma = \theta/\alpha$, and for the derivation of the shear stress from the measured torque.[7] In the domain of linear viscoelasticity, under a sinusoidal strain $\gamma(t) = \gamma_0(\sin \omega t)$ of amplitude γ_0 and pulsation ω, the elastic and loss moduli $G'(\omega)$ and $G''(\omega)$ are computed from the sinusoidal stress.[8] The determination of the domain of linear viscoelasticity is required before any analysis.

The RPA can also be operated in the relaxation mode, imposing a step strain of controlled amplitude γ and measuring the decrease of the shear stress $\sigma(t,\gamma)$ with time when this deformation is kept constant. This measurement yields another function characteristic of viscoelasticity, the relaxation modulus in shear, $G(t,\gamma) = \sigma(t,\gamma)/\gamma$. In practice, this measurement presents the following limitations. First, the data obtained at small strains and long times are scattered because small values of the measured torque fall below the sensibility threshold of the RPA (1 dNm). Second, with the RPA, the initial step strain is likely to be achieved within 0.05 s according to the manufacturer. However, for the larger strains ($\gamma > 5.6$), this is actually achieved in approximately 0.2 s, so the imposed deformation cannot be considered a pure step strain. Despite these limitations, we see later that measurements in the relaxation mode give satisfactory results for a specified time range and are particularly useful in the domain of nonlinear viscoelasticity.

Shear-stress-controlled rheometry with the SCR

A thorough description of the device used and of the testing procedure in creep can be found in previous articles.[4,9] The sample is enclosed in the annular cavity defined by two coaxial cylinders. Shearing of the material is promoted by a weight being hung on the inner cylinder, whose displacement is recorded with a micrometer-sensitive optical transducer. The shear stress σ is derived from the weight and geometrical parameters of the gap. In these experiments, a weight compensation device is used, consisting of a counterweight equilibrating the weight of the inner cylinder. It enables the stress to be as low as desired.

All the data processing for the determination of the viscosity function has been described elsewhere.[4] Here, the creep compliance is addressed, and it is derived from the recordings as follows. The position of the transducer, $p(t)$, is set to zero before the start of the run, that is, just before the weight is applied to the inner cylinder. The displacement recording is the evolution of $p(t)$ and consists of several thousands points at different time intervals. Short runs were performed over 800 s, with 4000 points being acquired every 0.2 s. In addition, long runs involved a first stage of data acquisition for 200 points every 0.1 s, instantaneously followed by a second set of 80 points every 1 s and a subsequent acquisition of over 3000 data points every 20 s for a total run duration of over 16 h. This experimental procedure allowed more tests to be performed and provided a wide range of data, the initial (800 s) part of the plots being often sufficient to assess the superposition (i.e., linear behavior) or not.

The total strain at time t is given by $\gamma(t) = 2p(t)/a \ln(b/a)$ (see the appendix). The creep compliance is obtained at a given stress σ from $J(t,\sigma) = \gamma(t,\sigma)/\sigma$. From the recordings, it could clearly be seen that an instantaneous strain occurred, so the compliance could be split into an instantaneous component and a delayed component. The compliance plotted in the subsequent graphs includes this instantaneous component and, therefore, exhibits a finite value at short times.

VISCOELASTIC BEHAVIOR OF FILLED ELASTOMERS

All rheological characterizations presented in this study were carried out at 100°C.

Strain-controlled behavior

A first discrimination between linear and nonlinear viscoelastic behaviors can be readily obtained with the RPA via oscillatory tests at a given angular frequency ω, with different strain amplitudes γ_0 imposed. The evolution of the measured elastic modulus $G'(\gamma_0)$ with strain amplitude γ_0 and for a pulsation $\omega = 6.28$ rad/s is shown in Figure 1(a) for the three samples under study. In all cases, a linear viscoelastic behavior corresponding to an elastic modulus independent of deformation can be observed at small deformations. In this deformation range, subsequent tests at a given strain amplitude and a varying angular frequency are performed, yielding the classical functions $G'(\omega)$ and $G''(\omega)$ of linear viscoelasticity. The evolution of the elastic modulus $G'(\omega)$ as a function of frequency ω at a strain amplitude $\gamma_0 = 0.07$ is shown in Figure 1(b) for the same three samples. In Figure 1(a), the critical deformation amplitude above which the elastic modulus decreases with increasing γ_0 characterizes the onset of the nonlinear viscoelastic behavior.

The influence of the filler content on the viscoelastic properties can be seen in Figure 1(a,b). A first observation concerns the critical deformation in Figure 1(a). It is a decreasing function of the filler content, indicating that the presence of the filler enhances the nonlinearity of the viscoelastic behavior. The dynamics of a

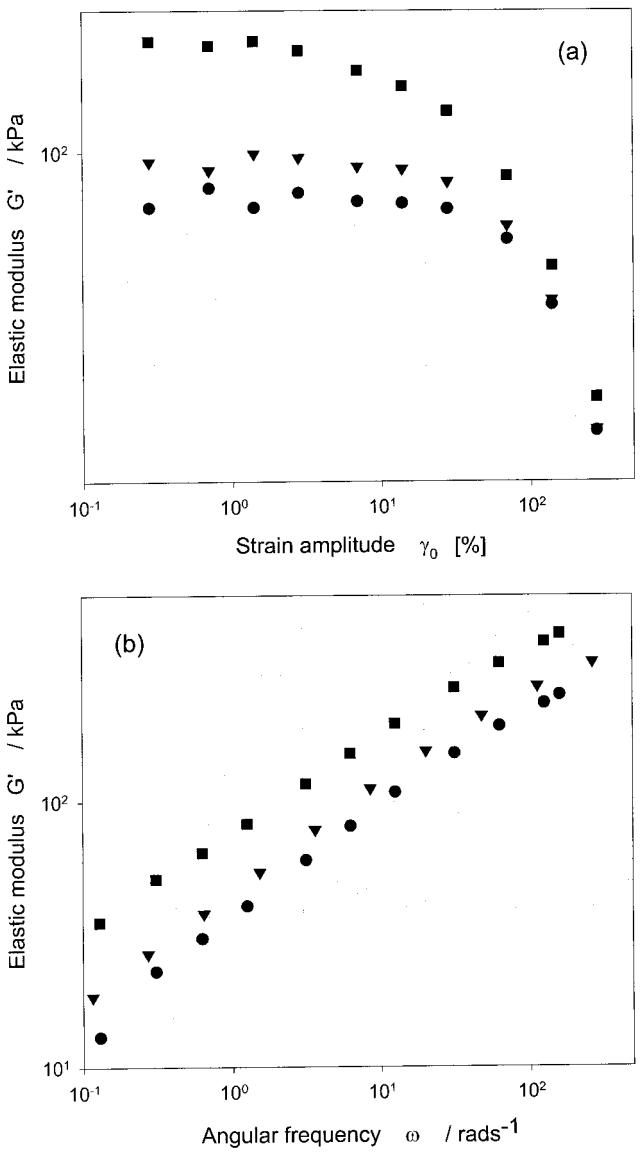

Figure 1 Evolution of the elastic modulus with (a) the strain amplitude (ω = 6.28 rad/s) and (b) the angular frequency (γ_0 = 0.07) for the three elastomer samples: (●) unfilled elastomer, (▼) elastomer filled with Φ = 0.045 carbon black, and (■) elastomer filled with Φ = 0.123 carbon black.

pure elastomer is dominated by the network formed by the entanglements between macromolecules, and this network can sustain large deformations. The incorporation of small particles into an elastomer promotes the formation of a new microstructure, which is more sensitive to the deformation than the pure elastomer network. In some cases, for highly filled elastomer compounds, no linear domain can be observed at all in the range of deformations accessible with the RPA. A second observation is that the increase of the filler volume fraction is associated, at a given oscillation amplitude [Fig. 1(a)] or frequency [Fig. 1(b)], with an increase in modulus. This effect is particularly significant in the domain of linear viscoelasticity. Moreover, it can be seen in Figure 1(b) that in the high-frequency range, the curves obtained at different volume fractions can be shifted by a numerical factor depending on the volume fraction only, as described, for instance, by the Guth and Gold equation.[10] At low frequencies, however, an additional mechanism, not elucidated yet, causes the modulus enhancement effect to become frequency-dependent; that is, here the filler content also causes a modification of the dynamics as such.

A second characterization of the compounds was made with the RPA in the relaxation mode, measuring the decrease of the shear stress $\sigma(t,\gamma)$ with time after a step deformation γ ranging from 0.07 to 12.6. As an example, the time evolution of relaxation moduli $G(t,\gamma)$ are shown in Figure 2 for the elastomer filled with a Φ = 0.123 carbon black volume fraction. The trends observed are the same as those for the other two compounds. For the smallest deformations ($\gamma \leq 0.14$), the relaxation moduli $G(t,\gamma)$ obtained at different deformations are identical within the experimental precision (with small scatter in the data when the measured torque is small, as mentioned earlier). This is characteristic of the domain of linear viscoelasticity, and the corresponding modulus is, therefore, the linear relaxation modulus in the limit of vanishing deformation, $G(t,\gamma = 0) = G_0(t)$, independent of deformation. For larger strains ($\gamma > 0.14$), a different curve is obtained for each deformation, the relaxation modulus at a given time decreasing with increasing deformation, which is a characteristic of the domain of nonlinear viscoelasticity. Note that the curves obtained at large strains ($\gamma > 5.6$) may not be significant,

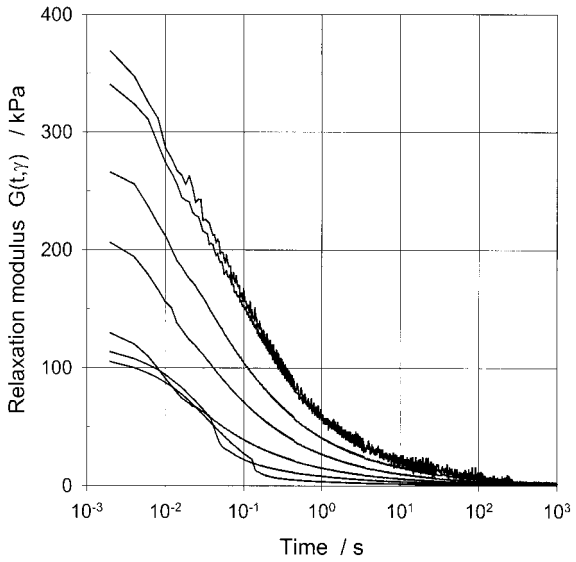

Figure 2 Time evolution of the relaxation modulus (elastomer filled with Φ = 0.123 carbon black) measured at different values of γ: 0.07, 0.14, 0.7, 1.4, 2.8, 5.6, and 12.6 (from top to bottom).

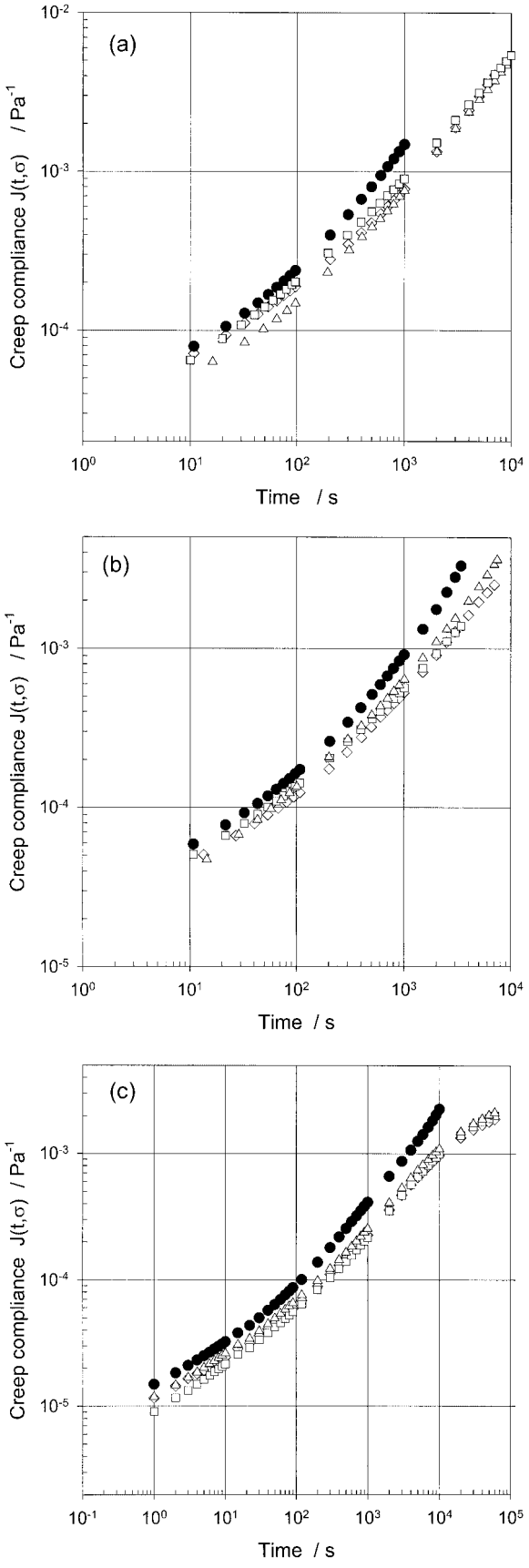

the imposed deformation being no pure step deformation as already mentioned. The range of step strains at which the transition between linear and nonlinear behaviors is observed is consistent with the range of deformation amplitudes showing the same transition in the oscillatory mode. An increase in the relaxation modulus with increasing filler content, at a given time and a given step strain, is also noticed (not shown here). The same previous interpretations can be made here concerning the influence of the filler content on the observed trends.

Stress-controlled behavior

Each compound was tested with the SCR in a number of runs under different stresses ranging from 500 to 20,000 Pa. In practice, the stress applied obviously had to be varied according to the filler content of the material because the resulting strain and experiment duration had to be kept within reasonable limits. Indeed, too low a stress level induced a very slow displacement, affecting the precision of the measurements. As a matter of fact, recordings of very slow displacements were very scattered because the variation of the position between two acquisition points was too close to the transducer precision. Moreover, a low shear stress resulted in excessive experimental duration (with respect to the material stability at a high temperature and possible maturation effects) for a steady flow to be attained. However, excessive stress resulted in very fast deformation and very large strains, quickly leading to damage (decohesion) to the sample. Therefore, a compromise was found, and the shear stress level was adapted to each compound; this explains why the ranges are not the same for all. For a given compound, the sample was changed at each run.

The plots of the creep compliance versus time for each compound, at the different stresses applied, are shown in Figure 3(a–c). The first comment that can be made concerns the level of the creep compliance, which decreases when the filler content increases, as expected. This is obviously correlated to the increase in the viscosity and dynamic moduli of the material. Next, for a given compound, the creep compliance increases as the shear stress increases, except for the lowest stress values. Indeed, the curves at low stress can be considered superposed within the experimen-

Figure 3 Time evolution of the creep compliance measured at different values of σ: (a) unfilled elastomer [(□) σ = 506 Pa, (△) σ = 765 Pa, (◇) σ = 1531 Pa, and (●) σ = 5783 Pa], (b) elastomer filled with Φ = 0.045 carbon black [(◇) σ = 506 Pa, (□) σ = 1084 Pa, (△) σ = 3036 Pa, and (●) σ = 5741 Pa], and (c) elastomer filled with Φ = 0.123 carbon black [(□) σ = 1446 Pa, (◇) σ = 2530 Pa, (△) σ = 3614 Pa, and (●) σ = 7590 Pa].

tal error interval, which is ±10% in the worst cases and most often ±5%. This clearly indicates that in this stress range, the compliance is only time-dependent and meets the requirement for the linear viscoelastic domain. Therefore, the linear domain is also apparent in these creep plots, although its evidence (stress-independent compliance) is different from what is observed in relaxation (stress-independent modulus). A trace of the yield behavior may be suspected in Figure 3(c) for the highest (in this work) filled compound (see the leveling out of the creep compliance at long times). However, when plotting the creep curves (deformation vs time), we do not see a clear transition between a solidlike behavior at low stresses and a fluidlike behavior at higher stresses. The deformation rates at long times are at least 10^{-5} s^{-1}, which can be considered significant, and are even 1 order of magnitude greater than those measured by other authors for highly filled compounds beyond the yield.[11] Another explanation for this effect is suggested later.

Conclusion

As can be stated from the two preceding sections, both the linear and nonlinear viscoelastic domains can be identified for the three batches used in this study and investigated by all the testing modes available. In the shear-controlled mode, the oscillatory tests provide the elastic and loss moduli of linear viscoelasticity together with the critical deformation amplitude above which the behavior becomes nonlinear, whereas the relaxation mode provides the shear-relaxation modulus not only in the linear viscoelasticity domain but also in the nonlinear domain. So do stress-controlled (creep) tests, yielding the compliance in the linear and nonlinear domains of viscoelasticity.

At this point, it would be interesting to establish a correspondence between these characteristic viscoelastic functions.

DERIVATION OF THE RELAXATION MODULUS FROM THE CREEP COMPLIANCE AND VICE VERSA

The purpose of this section is to correlate the data obtained from the RPA and SCR measurements. This can be achieved on two levels. In the domain of linear viscoelasticity, data processing based on a generalized Maxwell model yields the relaxation modulus $G_0(t)$ from the experimental creep compliance $J_0(t)$ via the intermediate computation of the relaxation spectrum.[12] A comparison with the relaxation experiments helps with evaluating the reliability and consistency of the two types of measurements. In the nonlinear viscoelastic domain, relaxation data are analyzed to characterize the strain dependence of the relaxation modulus. This allows for the determination of the so-called damping function, introduced in constitutive equations such as the K-BKZ model. This model provides, among other examples, a creep function depending on both time and stress, which is finally compared with the experimental compliance data.

Linear viscoelasticity

In this case, we extract the relaxation modulus from computations based on creep compliance data and compare them to experimental data. This requires the determination of the relaxation time spectrum $H(\lambda)$. For this, the experimental data are analyzed with a generalized Maxwell model.

Generalized maxwell model

In the range of small deformations, the relation between the deformation and stress in a viscoelastic material is described by the Boltzmann superposition principle:

$$\sigma(t) = \int_{-\infty}^{t} M(t - t') \cdot [\gamma(t) - \gamma(t')] \cdot dt' \qquad (1)$$

where $\sigma(t)$ and $\gamma(t)$ are the shear stress and strain at time t. $M(t - t')$ is the memory function of the linear viscoelasticity, which is deduced from the relaxation modulus $G_0(t)$:[8]

$$M(t - t') = \frac{d}{dt'} G_0(t - t') \qquad (2)$$

With such a model, it is necessary to represent the modulus by an explicit mathematical function, and the function most often used is that of the discrete generalized Maxwell model:

$$G_0(t - t') = \sum_{i=1}^{N} G_i \exp[-(t - t')/\lambda_i] \qquad (3)$$

where G_i is the elastic modulus of a simple Maxwell element corresponding to a relaxation time λ_i. Physically, this model is consistent with the fact that the relaxation of a polymeric material is the result of several independent relaxation processes at the molecular level, each having a characteristic time λ_i. The discrete relaxation spectrum, that is, the set of N pairs of values (G_i,λ_i), is determined from experimental data. The generalized Maxwell model is attractive from a practical point of view because it allows the use of a large number N of relaxation modes. This is necessary when we are dealing with polymers of large polymolecularity, as is the case in this study. As a counterpart, the

determination of the discrete spectrum is an ill-posed problem, which means that an infinite number of sets of N relaxation modes can be found that are equally satisfactory from the point of view of fitting the data. Honerkamp and Weese[13] explored some of the problems associated with the determination of the discrete spectrum as a material characteristic, for example, for comparison with a spectrum calculated from a molecular theory.

Computation of the relaxation time spectrum

The relaxation function $H(\lambda)$ and the retardation function $L(\lambda)$ can be computed from a set of discrete data of either the dynamic moduli $G'(\omega)$ and $G''(\omega)$ or the relaxation modulus $G_0(t)$ or even the creep function $J_0(t)$ (for more details on the relationships between these functions in the framework of the Maxwell model, see ref. 12). In the literature, various techniques have been proposed to determine the discrete relaxation spectrum (G_i,λ_i) from either a set of storage and loss modulus data or any other viscoelastic function. Among these, we chose a nonlinear regularization[14] method (NLREG[15]). Of course, the time range of the relaxation spectrum determined by NLREG does not extend beyond the time range of the set of data. In practice, we used the recommended number of modes $N = 71$ for all the computations. To validate the program, we first converted experimental sets of $G'(\omega)$ and $G''(\omega)$ data, via the determination of $H(\lambda)$, into the relaxation modulus $G_0(t)$. An excellent superposition between measured and computed $G_0(t)$ values was obtained in the 0.01–100-s time range in which the relaxation experiments are reliable. This calculated $G_0(t)$ is not scattered and, therefore, is used instead of experimental $G_0(t)$ for further computation and plotting (see Fig. 4 for an example). It can be concluded that the linear viscoelastic approach that was originally developed for pure polymer systems also applies very satisfactorily to the more complex systems that we have tested.

From the creep compliance data to the relaxation modulus

$J_0(t)$ data measured in the linear domain are now processed by NLREG to derive $H(\lambda)$ and ultimately $G_0(t)$. These computed data are plotted in Figure 4, in which it is clear that the data obtained with the RPA and SCR concern very different time ranges (0.001–20 s for the RPA and 1–≥1000 s for the SCR). However, the agreement between the two sets of data is satisfactory for the time range in which their time domains overlap. The interest in the confrontation of both techniques is that it allows us to extend the time range actually available for each.

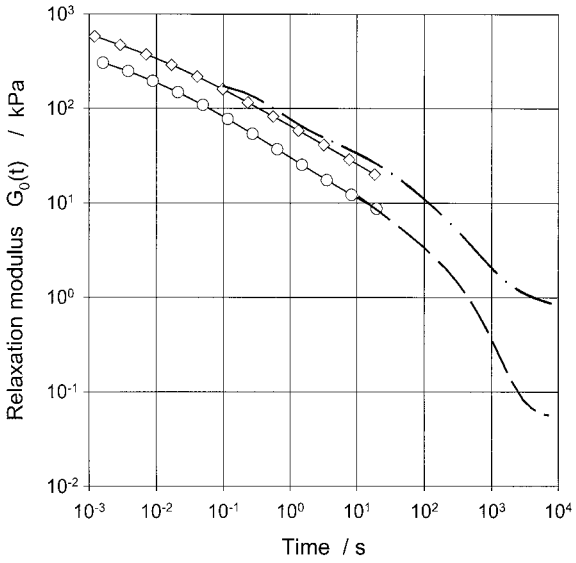

Figure 4 Time evolution of the linear relaxation modulus computed with NLREG from $G'(\omega)$ and $G''(\omega)$ measured with the RPA [(○) unfilled elastomer and (◇) elastomer filled with $\Phi = 0.123$ carbon black] and from $J_0(t)$ measured with the SCR [(–) unfilled elastomer and (- · -) elastomer filled with $\Phi = 0.123$ carbon black].

Nonlinear viscoelasticity

In this part, we show how, starting from the relaxation modulus data obtained in the nonlinear viscoelasticity domain, it is possible to derive a nonlinear viscoelastic model of type K-BKZ. This model is then used to compute the creep compliance data obtained in the nonlinear viscoelasticity domain.

Analysis of relaxation modulus data

When Figure 2 is plotted on a log–log scale, the curves of the relaxation modulus obtained at different deformations can be deduced from one another by a simple vertical shift. This suggests the following procedure. We divide the modulus obtained at a given deformation $G(t,\gamma)$ by a quantity that depends on the deformation, which is denoted $h(\gamma)$. This quantity is chosen in such a way that the division yields the modulus of linear viscoelasticity, $G_0(t)$. The result is shown in Figure 5 on a semilog scale by the plotting of $G(t,\gamma)/h(\gamma)$: all the curves of Figure 2 collapse on a single curve corresponding to $G_0(t)$. Note, however, that in Figure 5, the collapsing does not work well at very short times ($t < 0.01$ s). For the rest of the time range, the nonlinear relaxation modulus can, therefore, be written as the product of a function of time by a function of deformation:

$$G(t, \gamma) = G_0(t) \cdot h(\gamma) \tag{4}$$

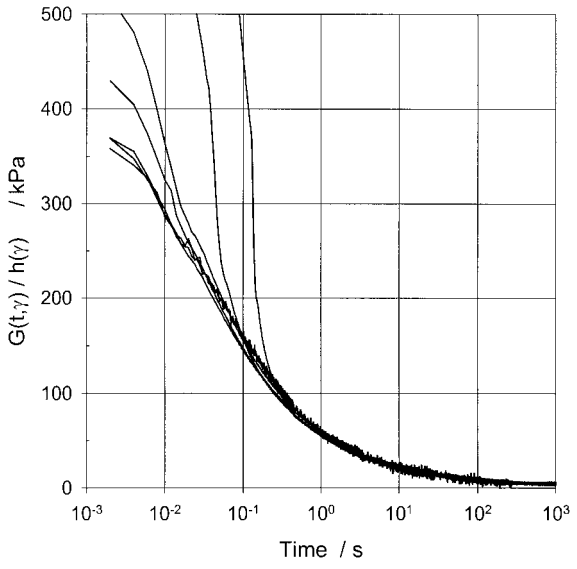

Figure 5 Master curve of $G(t,\gamma)/h(\gamma)$ as a function of time (elastomer filled with $\Phi = 0.123$ carbon black) at different values of γ: 0.07, 0.14, 0.7, 1.4, 2.8, 5.6, and 12.6 (from bottom to top).

where $h(\gamma)$ is called the damping function. The property described by eq. (4) is called the factorization property and expresses the fact that the effects of time and deformation on the relaxation process are independent. This was experimentally observed long ago for a wide range of pure polymers.[16,17] It was also predicted by molecular theories showing that it originates from a loss of entanglements as the strain amplitude increases.[18] The theories also show that this property does hold only for a time range beyond a characteristic molecular time. The striking point in our work is that we observe the factorization property not only for the pure elastomer but also for the two filled compounds. In other words, for the relatively low level of filler content studied here, the elastomer dynamics in the nonlinear domain is not qualitatively modified by the presence of the particles. Only the values of the damping function are affected by the filler content. In Figure 6, we have plotted the evolution of damping functions with deformation γ. Each point of $h(\gamma)$ has been obtained from a relaxation modulus at a given value of γ by the procedure described previously. For the sake of clarity, only the pure elastomer and the more filled compound are represented. The damping function starts from $h(\gamma) = 1$ in the linear domain (of vanishing deformation) and decreases with increasing strain. The values of $h(\gamma)$ at a given deformation are smaller for a larger filler volume fraction. This indicates that the sensitivity to deformation increases with increasing filler content.

Nonlinear integral viscoelastic model: the factorized K-BKZ model

The property of factorization that has been shown experimentally in the previous section leads us to use a nonlinear viscoelastic model of type K-BKZ.[8] This is a factorized integral model for which the shear stress at time t is written as follows:

$$\sigma(t) = \int_{-\infty}^{t} M(t - t') \cdot h[\gamma(t) - \gamma(t')] \cdot [\gamma(t) - \gamma(t')] \cdot dt' \quad (5)$$

This model is a generalization of the Boltzmann superposition principle, in which the nonlinearity is introduced via the damping function. [Equation (1) is recovered for vanishing deformation as $h(\gamma) = 1$]. Equation (5) can be conveniently rewritten as follows:

$$\sigma(t) = G_0(t) \cdot h[\gamma(t)] \cdot \gamma(t) + \int_0^t \frac{d}{dt'} G_0(t - t') \cdot h[\gamma(t) - \gamma(t')] \cdot [\gamma(t) - \gamma(t')] \cdot dt' \quad (6)$$

Under this form, the K-BKZ model is easily handled to compute the stress from a given deformation history, with both the linear relaxation modulus and the damping function being known. For instance, for an imposed step strain [$\gamma(t) = \gamma$ for $t > 0$], eq. (6) readily yields eq. (4). More difficult, however, is its application to the creep tests because in eq. (6) the unknown deformation becomes an implicit function of the im-

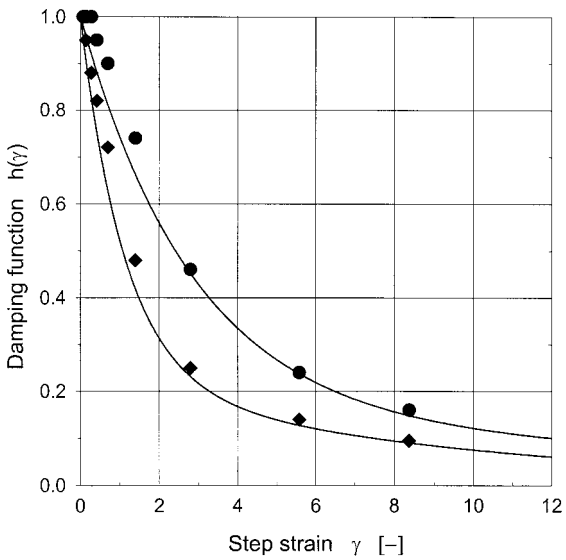

Figure 6 Evolution of the damping function with the step strain [(●) unfilled elastomer and (♦) elastomer filled with $\Phi = 0.123$ carbon black]. The lines show the fit by a function of the form $h(\gamma) = A \exp(-\alpha\gamma) + B \exp(-\beta\gamma)$.[20]

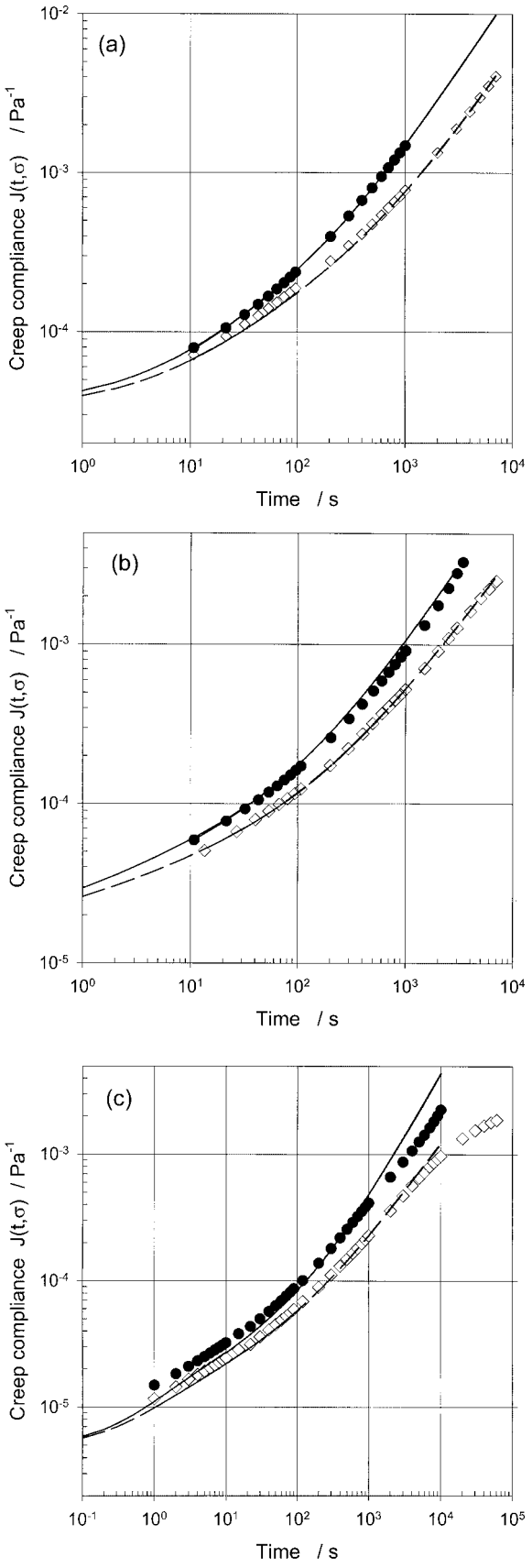

posed stress. This difficulty can be solved numerically with the procedure used by Wagner[19] in a previous work on low-density polyethylene melts in extensional creep. The integral equation with the unknown deformation is inverted numerically by a method of successive integration on constant time steps. In practice, we choose the time step in relation to the experimental creep data acquisition period described in the Experimental section. We use for $G_0(t)$ the 71 relaxation modes computed by NLREG from the creep compliance data. For computational tractability, the measured damping functions have to be fitted by analytical equations. We have used for that an equation of the Osaki type[20] (the result of the fit is shown as continuous lines in Fig. 6).

Comparison with creep compliance data

The results of the computation are shown in Figure 7 (continuous lines) along with the experimental data (which are the same as those in Fig. 3). On each graph, the creep compliance corresponding to the linear domain (vanishing stress) is well predicted by the solution of eq. (6), for which we have taken $h(\gamma) = 1$. This is simply a consequence of the consistency of the Maxwell model, as the spectrum of relaxation times used in eq. (6) has been deduced from this same creep compliance. A small deviation of the Maxwell model from the experimental data can be observed for the highest filled compound [Fig. 7(c)], but we attribute this to some problems with the experimental data at very long times, as discussed later. Concerning the description of the nonlinear creep compliance (measured at a large stress), it can be seen that for the pure elastomer [Fig. 7(a)] the K-BKZ model is in very good agreement with the experimental data, at least in the time range investigated here. For the lowest filled compound [Fig. 7(b)], the agreement is also good, despite a small deviation observed from $t > 200$ s. For the more filled compound [Fig. 7(c)], the agreement is only qualitative, a discrepancy between the model and experiment arising already at short times. In all cases, the model succeeds in describing the increase of creep compliance with increasing stress. This is achieved essentially through the damping function. However, a quantitative agreement generally appears to become more difficult at long times, at which the model tends to overestimate the creep compliance. This is due to

Figure 7 Time evolution of the creep compliance at different values of σ [(●,◇) measured with the SCR (see Fig. 3), (—) computed with the K-BKZ model, and (–) computed with the generalized Maxwell model]. For the modeling, the relaxation spectrum was computed from $J_0(t)$ measured in the linear domain: (a) unfilled elastomer, (b) elastomer filled with $\Phi = 0.045$ carbon black, and (c) elastomer filled with $\Phi = 0.123$ carbon black.

limitations of the nonlinear K-BKZ model under the form used in this work, limitations that are discussed next.

CONCLUSIONS

The cross-check method used in the domain of linear viscoelasticity has been validated for the three batches with equivalent quantitative agreement. The implementation of the K-BKZ model in the domain of nonlinear viscoelasticity yields quantitatively good results for the pure polymer [Fig. 7(a)], whereas the agreement between the experiment and model deteriorates with increasing filler volume fraction [Fig. 7(b,c)]. This raises a number of comments.

The first remark concerns the precision achieved in the measurement of the different material functions. Relatively large experimental errors in the measurements of the relaxation modulus at very long times (due to the limits of the RPA torque transducer) have already been mentioned. Moreover, the step strain becomes questionable at large strains. As a result, the time and deformation domain over which the damping function can be considered valuable is restricted, too. Problems have also been noticed with the measurements of compliance from SCR tests at the very beginning of the test run. The displacement is all the smaller as the stress is small. Then, for the lowest stress values, the accuracy of the measurement is close to the displacement transducer sensitivity, and erratic variations can be observed. In these situations, the relative experimental error for the initial values of compliance is large.

Another experimental difficulty can be observed at the end of some experimental SCR recordings [particularly with the more filled compound; see Fig. 3(c)]. The compliance seems to level out, especially when the run is long, that is, greater than about 6 h. A tendency to yielding may be invoked, but as mentioned earlier, because of the magnitude of the deformation rate, it is difficult to conclude that no flow occurs. The shape of the creep plot at long times may also indicate a problem of maturation (or aging) of the compound. As a matter of fact, carbon black/rubber compounds are known to have their rheological properties evolving over the first weeks of their storage, and these properties evolve all the faster (i.e., within hours) when the temperature is high.[21] Such behavior is related, in the case of SBR compounds, to the increase in the bound rubber fraction. Therefore, despite the long storage time observed before the testing of the materials, a residual maturation effect in the SCR may not be excluded. This interpretation is consistent with the fact that the compliance leveling out is not observed here with the lowest filled compounds.

From a more fundamental point of view, the question of the flow mechanisms in such filled elastomer compounds is addressed through our experiments. What type of molecular dynamics is involved in the linear and nonlinear viscoelastic shear behavior of those filled polymeric materials is not elucidated yet. In particular, although the property of factorization seems here to hold as for pure polymers, the physical significance of a damping function for filled elastomers has to be further examined.

In conclusion, this study is interesting first because it shows the processing of quite original experimental data, obtained on complex polymeric materials, for cross-checking material functions extracted from different types of rheological techniques and second because it raises a number of more fundamental questions that need to be further considered.

APPENDIX: DERIVATION OF THE DEFORMATION FROM THE SCR DISPLACEMENT RECORDINGS

From the displacement curve, the inner cylinder velocity is calculated as follows:

$$v(t) = \frac{dp(t)}{dt}$$

The shear rate $\dot{\gamma}(t)$ is derived from the value of $v(t)$ with the annular geometry of the gap taken into account. $\dot{\gamma}$ is given as follows:

$$\dot{\gamma}(t) = \frac{2v(t)}{a \ln \frac{b}{a}}$$

where a and b are the inner and outer diameters of the annular gap, respectively.

The shear rate is defined as the derivative of the strain function $\gamma(t)$. Then, it can be written that

$$\dot{\gamma}(t) = \frac{d\gamma(t)}{dt} = \frac{2v(t)}{a \ln \frac{b}{a}} = \frac{2\,dp(t)}{a \ln \frac{b}{a}\,dt}$$

The total strain at time t is

$$\gamma(t) = \int_0^t \frac{d\gamma}{dt'}\,dt' = \int_0^t \frac{2}{a \ln \frac{b}{a}}\,dp$$

Therefore,

$$\gamma(t) = \frac{2}{a \ln \frac{b}{a}}[p(t')]_0^t = \frac{2}{a \ln \frac{b}{a}}\,p(t)$$

References

1. Leonov, A. I. J Rheol 1990, 34, 1039.
2. Joshi, P. G.; Leonov, A. I. Rheol Acta 2001, 40, 350.
3. Pawlowski, H.; Dick, J. Rubber World 1992, 206, 35.
4. Barrès, C.; Leblanc, J. L. Polym Test 2000, 19, 177.
5. Vinogradov, G. V.; Plotnikova, E. P.; Zabugina, M. P.; Borisenkova, E. K. Rheol Acta 1988, 27(Suppl.), 382.
6. Osanaiye, G. J.; Leonov, A. I.; White, J. L. Rubber Chem Technol 1995, 68, 50.
7. Mongruel, A. Proceedings of the 8th International Seminar on Elastomers, Le Mans, France, 2001.
8. Bird, R. B.; Armstrong, R. C.; Hassager, O. Dynamics of Polymeric Liquids; Wiley: New York, 1987; p 18.
9. Barrès, C.; Leblanc, J. L.; Guilet, S. Polym Test 2001, 20, 329.
10. Guth, E.; Gold, O. Phys Rev 1938, 53, 332.
11. Simhambhatla, M.; Leonov, A. I. Rheol Acta 1995, 34, 329.
12. Ferry, J. D. Viscoelastic Properties of Polymers, 3rd ed.; Wiley: New York, 1980; Chapter 3.
13. Honerkamp, J.; Weese, J. Macromolecules 1989, 22, 4372.
14. Honerkamp, J.; Weese, J. Rheol Acta 1993, 32, 65.
15. NLREG (software); University of Freiburg: Freiburg, Germany.
16. Wagner, M. H. Rheol Acta 1976, 15, 136.
17. Osaki, K.; Nishizawa, K.; Kurata, M. Macromolecules 1982, 15, 1068.
18. Doï, M.; Edwards, S. F. The Theory of Polymer Dynamics; Clarendon: Oxford, 1986.
19. Wagner, M. H. J Non-Newtonian Fluid Mech 1978, 4, 39.
20. Osaki, K. Proceedings of the 7th International Congress on Rheology; Klason, C.; Kubat, J., Eds.; Chalmers University of Technology: Gothenburg, Sweden, 1976; p 104.
21. Leblanc, J. L. Kautsch Gummi Kunstst 2001, 54, 327.